Universiteit
Leiden
The Netherlands

Exploration of the endocannabinoid system using metabolomics

Di, X.

Citation
Di, X. (2023, February 7). *Exploration of the endocannabinoid system using metabolomics*. Retrieved from https://hdl.handle.net/1887/3515754

Version:	Publisher's Version
License:	Licence agreement concerning inclusion of doctoral thesis in the Institutional Repository of the University of Leiden
Downloaded from:	https://hdl.handle.net/1887/3515754

Note: To cite this publication please use the final published version (if applicable).

Chapter 2

A platform for the analysis of metabolites in endocannabinoids - related pathways.

Based on

Xinyu Di, Wouter P.F. Driever, Corné van der Plas, Zhengzheng Zhang, Timo Wendel, Tom van der Wel, Amy Harms, Elke H.J. Krekels, Mario van der Stelt, Isabelle Kohler, Thomas Hankemeier

A platform for the analysis of metabolites in endocannabinoids - related pathways.

Manuscript in preparation

Abstract

The endocannabinoid system (ECS) is a widely-distributed signaling system, which is involved in multiple physiological processes and targeted for the treatment of many diseases. However, due to the wide distribution and intrinsic complexity of the ECS, clinical success targeting this system is limited. To monitor the change of the ECS under pathological conditions and pharmacological modulations, a liquid chromatography-mass spectrometry (LC-MS) method was developed for the profiling of the ECS associated metabolites. This method enabled the analysis of endocannabinoids and more than 100 related metabolites, including *N*-acyl-phosphatidylethanolamines (NAPEs), 2-lyso-*N*-acyl-phosphatidylethanolamines (lyso-NAPEs), glycerol-phospho-acylethanolamines (GP-NAEs), free fatty acids (FFAs), which covered the metabolic pathways of *N*-acyl ethanolamines (NAEs). The method has been optimized and validated for mice brain samples, which enables the screening of enzymes potentially involved in the ECS in genetically modulated mice models.

1. Introduction

The endocannabinoid system (ECS) is a signaling system composed of the cannabinoid receptors (CBR) type 1 (CB1R) and type 2 (CB2R), anandamide (AEA) and 2-arachidonoyl glycerol (2-AG), as well as several metabolic enzymes[1,2]. CB1R and CB2R were first identified during the investigation of the psychoactive cannabinoid found in marijuana (tetrahydrocannabinol, THC)[3]. Then, AEA and 2-AG were found to be the major endogenous agonists of the CBRs and defined as endocannabinoids (eCBs)[4,5]. In addition to these two eCBs, their structural analogues do not have affinity for CB1R or CB2R but are also playing important roles in ECS signaling[1,6]. These eCB analogues include other *N*-acyl ethanolamines (NAEs), such as palmitoylethanolamine (PEA), oleoylethanolamine (OEA), and linoleylethanolamine (LEA), as well as other 2-acylglycerols (2-AcGs), such as 2-linoleoylglycerol (2-LG) and 2-oleoylglycerol (2-OG)[6].

The NAEs and 2-AcGs are generated from separate pathways. Generally, the synthesis of NAEs begins with the generation of *N*-acyl-phosphatidylethanolamines (NAPEs) from membrane phosphatidylethanolamines (PEs) and other phospholipids, involving *N*-acetyltransferases from the phospholipase A and acyltransferase (PLAAT) family and calcium-dependent phospholipase A2 (PLA2) subfamily[1,7,8]. Then, NAEs are generated from NAPEs directly by *N*-acyl phosphatidylethanolamine phospholipase D (NAPE-PLD), or via other intermediate metabolites, such as 2-lyso-*N*-acyl-phosphatidylethanolamines (lyso-NAPEs), glycerol-phospho-acylethanolamines (GP-NAEs)[1,2,7]. The NAEs are further metabolized by fatty acid amide hydrolase (FAAH) or *N*-acylethanolamine-hydrolyzing acid amidase (NAAA) into free fatty acids (FFAs) and ethanolamine[1,7]. On the other hand, the 2-AcGs are mostly generated from diacylglycerols (DAGs) by diacyl-glycerol lipase (DAGL), other precursors such as lysophosphatidic acids (LPAs) are also involved[9,10]. The degradation of 2-AcGs is mostly catalyzed by monoacylglycerol lipase (MAGL), other metabolic enzymes include α,β-hydrolase 6 and 12 (ABHD 6&12)[11]. The downstream metabolites of 2-AcGs are glycerol and FFAs.

Most of the previous studies regarding the ECS looked at the change of endocannabinoids, and sometimes their analogues[12–15]. While a better coverage of the related metabolites gives more relevant information, especially when studying the role of potential metabolic

enzymes, and when assessing the pharmacological roles of inhibitors targeting the metabolic enzymes. Liquid chromatography - mass spectrometer (LC-MS) methods that covers these ECS-related metabolites have been reported[16–19]. However, these methods measured these metabolites in separated LC-MS runs and sometimes used separate sample preparations[16–19], which lowered the efficiency and probably introduced more systematic errors. Therefore, we aimed to develop a platform that covers the wide range of ECS - related metabolites, by using one sample preparation and one LC-MS run.

2. Material and methods

2.1 Solvents and standards

Purified water was produced using a Milli-Q PF Plus system (Merck Millipore, Burlington, Massachusetts, United States). LC-MS-grade acetonitrile (ACN), isopropanol (IPA), chloroform ($CHCl_3$) and formic acid were purchased from Biosolve B.V. (Valkenswaard, Netherlands). Anhydrous methyl tert-butyl ether (MTBE, ≥99.8%), ammonium acetate (≥99.0%) and ammonium formate (≥99.9%) were purchased from Sigma-Aldrich (St. Louis, Missouri, United States). Anhydrous butanol (BuOH) was purchased from thermo scientific (Waltham, Massachusetts, United States).

Standard reagents 1-Arachidonoylglycerol (1-AG), 2-Arachidonoylglycerol (2-AG), 1-Linoleoyl Glycerol (1-LG), 2-Linoleoyl Glycerol (2-LG), 1-Oleoyl Glycerol (1-OG), 2-Oleoyl Glycerol (2-OG), Anandamide (AEA), Docosahexaenoyl Ethanolamide (DHEA), Linoleoyl Ethanolamide (LEA), α-Linolenoyl Ethanolamide (α-LEA), Palmitoleoyl Ethanolamide (POEA), Pentadecanoyl Ethanolamide (PDEA), Dihomo-γ-Linolenoyl Ethanolamide (DGLEA), Mead acid Ethanolamide (ETAEA), Docosatetraenoyl Ethanolamide (DEA), Oleoyl Ethanolamide (OEA), Palmitoyl Ethanolamide (PEA), Stearoyl Ethanolamide (SEA), Eicosapentaenoyl Ethanolamide (EPEA) and deuterated internal standards 5Z,8Z,11Z,14Z-eicosatetraenoic-5,6,8,9,11,12,14,15-d8 acid (2-AG-d8), *N*-(2-hydroxyethyl)-5Z,8Z,11Z,14Z-eicosatetraenamide-5,6,8,9,11,12,14,15-d8 (AEA-d8), *N*-(2-hydroxyethyl-1,1',2,2'-d4)-4Z,7Z,10Z,13Z,16Z,19Z-docosahexaenamide (DHEA-d4), *N*-(2-hydroxyethyl-1,1,2,2-d4)-9Z,12Z-octadecadienamide (LEA-d4), *N*-(2-hydroxyethyl-1',1,2,2'-d4)-9Z-octadecenamide (OEA-d4), *N*-(2-hydroxyethyl)-hexadecanamide-7,7,8,8-d4 (PEA-d4) and *N*-(2-hydroxyethyl)-octadecanamide-18,18,18-d3 (SEA-d3) were

purchased from Cayman Chemical (Ann Arbor, Michigan, United States). Ammonium salts of 1,2-Dioleoyl-sn-glycero-3-phospho (*N*-palmitoyl) ethanolamine (18:1, 18:1-PE-N-16:0), 1,2-Dioleoyl-sn-glycero-3-phospho (*N*-heptadecanoyl) ethanolamine (18:1, 18:1-PE-N-17:0), 1,2-Dioleoyl-sn-glycero-3-phospho (*N*-oleoyl) ethanolamine (18:1, 18:1-PE-N-18:1), 1,2-Dioleoyl-sn-glycero-3-phospho (*N*-arachidonoyl) ethanolamine (18:1, 18:1-PE-N-20:4), 1-(1Z-octadecenyl)-2-oleoyl-sn-glycero-3-phospho (*N*-palmitoyl) ethanolamine (p18:0, 18:1-PE-N-16:0), 1-(1Z-octadecenyl)-2-oleoyl-sn-glycero-3-phospho (*N*-heptadecanoyl) ethanolamine (p18:0, 18:1-PE-N-17:0), 1-(1Z-octadecenyl)-2-oleoyl-sn-glycero-3-phospho (*N*-oleoyl) ethanolamine (p18:0, 18:1-PE-N-18:1), 1-(1Z-octadecenyl)-2-oleoyl-sn-glycero-3-phospho (*N*-arachidonoyl) ethanolamine (p18:0, 18:1-PE-N-20:4), 1-oleoyl-2-hydroxy-sn-glycero-3-phospho (*N*-palmitoyl) ethanolamine (18:1, OH-PE-N-16:0), 1-oleoyl-2-hydroxy-sn-glycero-3-phospho (*N*-heptadecanoyl) ethanolamine (18:1, OH-PE-N-17:0), 1-oleoyl-2-hydroxy-sn-glycero-3-phospho (*N*-oleoyl) ethanolamine (18:1, OH-PE-N-18:1), 1-oleoyl-2-hydroxy-sn-glycero-3-phospho (*N*-arachidonoyl) ethanolamine (18:1, OH-PE-N-20:4), 1-(1Z-octadecenyl)-2-hydroxy-sn-glycero-3-phospho (*N*-palmitoyl) ethanolamine (p18:0, OH-PE-N-16:0), 1-(1Z-octadecenyl)-2-hydroxy-sn-glycero-3-phospho (*N*-heptadecanoyl) ethanolamine (p18:0, OH-PE-N-17:0), 1-(1Z-octadecenyl)-2-hydroxy-sn-glycero-3-phospho (*N*-oleoyl) ethanolamine (p18:0, OH-PE-N-18:1), 1-(1Z-octadecenyl)-2-hydroxy-sn-glycero-3-phospho (*N*-arachidonoyl) ethanolamine (p18:0, OH-PE-N-20:4) were synthesized as previously described.

2.2 Preparation of standards stock solutions and internal standards stock solutions

Purchased or synthesized standards/internal standards(IS) were dissolved in ethanol, chloroform or ACN at different stock concentrations. These stock solutions were further diluted and mixed to make the standard stock solutions and IS stock solutions. Standard stock solution I contained eCBs and eCB analogues. Standard stock solution II contained FFAs. Standard stock solution III contained NAPEs, pNAPEs, lyso-NAPEs and lyso-pNAPEs. IS stock solution A contained the deuterated form of eCBs and eCB analogues. IS stock solution B contained the deuterated form of FFAs. IS stock solution C contained 18:1, 18:1-PE-N-17:0, p18:1, 18:1-PE-N-17:0, 18:1-OH-PE-N-17:0, p18:1-OH-PE-N-17:0, OH-OH-PE-N-17:0 and DAG(15:0, 15:0). The concentrations of standard stock solutions and IS stock solutions were detailed in **Table S1** and **Table S2**, respectively. Standard stock

solution I, II and IS stock solution A, B were stored at -80 °C, Standard stock solution III and IS stock solution C were stored at -20 °C.

2.3 Preparation of calibration standard solutions and internal standard work solutions

The standard stock solution I, II, III were mixed to make a C10 calibration standard solution, the dilution ratios were 5, 13.5 and 13.5, respectively. The C10 calibration standard solution was further diluted by series of two-fold dilutions to make the other 9 calibration standard solutions. C0 calibration standard solution was the ACN used for the dilution. The IS stock solution A and B were mixed to make a IS work solution, the dilution ratio was 10.

2.4 Profiling of fragmentation patterns.

Individual standard stock solutions of NAPEs, pNAPEs, lyso-NAPEs, and lyso-pNAPEs were diluted to 10μM and infused using a syringe pump into a SCIEX TripleTOF 5600 mass spectrometer (AB Sciex, Framingham, MA, USA). Electrospray ionization (ESI) was carried out in positive and negative mode, with the following ESI parameters: source temperature, 600 °C; Gas 1 (nebulizer gas), 0 L/min; Gas 2 (heater gas), 15 L/min; curtain gas, 20 L/min; collision gas, medium; ion spray voltage, 5500V for positive and -4500V for negative. The Q1 scan mode was used for searching the precursor ions, while the product ion mode with the collision energy (CE) ranging from -10 V to -100 V was used in searching for the product ions.

2.5 Sample preparation

Brain lysates (1mg protein/mL, 100 μL) were thawed on ice in 1.5 mL Eppendorf tubes. To each sample 10 μL IS work solution was added, followed by 100 μL extraction buffer (0.2 M citric acid and 0.1 M disodium hydrogen phosphate, pH 4) and 1000 μL extractant (MTBE:BuOH, 50:50, v/v). Samples were then mixed in a Next Advance Bullet Blender (5 min, 90% speed, room tempreture) followed by centrifugation (16,000 x g, 10 min, 4°C). 950 μL of the organic layer was transferred into clean, pre-cooled tubes and concentrated in a SpeedVac vacuum concentrator (ThermoFisher Scientific, Waltham, USA), followed by adding 50 μL of reconstitution solution (BuOH:ACN, 50:50, v/v) and agitating for 15 min. The reconstituted samples were centrifuged (16,000 g, 10 min, 4ºC) and 40 μL were transferred into autosampler vials with inserts. Samples were kept at 7°C in the autosampler for less than 24 hours before analysis.

2.6 LC-MS/MS conditions

Extracted samples were analyzed using a Shimadzu LC system (Shimadzu Corporation, Kyoto, Japan) hyphenated with a SCIEX QTRAP 6500+ mass spectrometer (AB Sciex, Framingham, MA, USA). The injection volume was 10μL. The separation was performed in a BEH C8 column (50 mm × 2.1 mm, 1.7 μm) from Waters Technologies (Mildford, MA, USA) maintained at 40°C, with the flow rate at 0.4 mL/min. The mobile phase was consisted of 2 mM $HCOONH_4$, 10 mM formic acid in water (A), ACN (B), IPA (C). The gradient was the following: starting conditions 20% B and 20% C; increase of B from 20% to 40% between 1 min and 2 min; maintaining B at 40% and C at 20% between 2 min and 7 min; increase of C from 20% to 50% between 7 min and 8 min; maintaining B at 40% and C at 50% between 8 min and 10 min; returning to initial conditions at 10.5 min and re-equilibration for 1.5 min. Electrospray ionization (ESI)-MS acquisition was carried out in positive and negative mode, with the following ESI parameters: source temperature, 600 °C; Gas 1 (nebulizer gas), 50 L/min; Gas 2 (heater gas), 50 L/min; curtain gas, 30 L/min; collision gas, medium; ion spray voltage, 4500V for positive and -4500V for negative. Selected reaction monitoring (SRM) was used for data acquisition.

2.7 Identification of metabolites using retention time mapping

For the identification of the metabolites (i.e. NAPEs, pNAPEs, lyso-NAPEs, lyso-pNAPEs), a screening approach based on the retention time (RT) mapping was used. The RTs of metabolites from one class can be linearly correlated with their total carbon number and double bond number: $RT = b0 + b1 \cdot carbon\ number + b2 \cdot double\ bond\ number$. For each class, 3 to 4 standards (including one internal standard) with different carbon numbers and double bond numbers were synthesized. Multiple regression were performed between RTs of these 4 standards with their corresponding carbon numbers and double bond numbers. Thus, the b0, b1 and b2 for each class of metabolites were calculated. Then, for each fatty acid chain on the N-position (i.e., *N*-palmitoyl, *N*-stearyl, *N*-oleoyl, *N*-linoleoyl, *N*-arachidonoyl, *N*-docosahexaenoyl), possible combinations of fatty acid chains (palmitoyl, stearyl, oleoyl, linoleoyl, arachidonoyl) on sn-1 and/or sn-2 position were listed. The carbon numbers and double bond numbers for each possible analyte were obtained and their theoretical RTs were calculated. Peaks from their specific MS transitions were integrated at the theoretical RTs. The peaks were identified as quantifiable analytes when 1) peaks existed

both of the two/three specific transitions; 2) the actual RT does not deviate more than 0.1 min from the calculated RT; 3) peak shape is good.

2.8 Method validation

Linearity The linearity within the calibration range was investigated with calibration lines (n=3 in the first batch, n=1 in the second and third batch). Calibration samples were prepared by spiking calibrations standards (C0 - C9) into brain lysate samples (1mg protein/mL, 100 μL). All the calibration lines were fitted to a non-weighted linear regression model.

Precision The within-run and between-run precisions samples were unspiked brain lysates (n=5) and spiked brain lysates at C8 level (n=5) over three separate batches. Within-run precision was calculated as the RSD of the peak area ratio of the precision samples from day 1 (n=5). Between-run precision was calculated as the RSD of the peak area ratio of the precision samples from all three batches (n=15).

Recovery and matrix effect Recovery and matrix effect were evaluated by spiking IS solutions [low level(C3), medium level(C5) and high level(C8)] into brain lysate samples (n=5). Recovery was the ratio of ISTD peak areas acquired from brain lysate samples with IS solutions spiked-before and spiked-after extraction. Matrix effect was the ratio of ISTD peak areas acquired from brain lysate samples with IS solutions spiked-after extraction and academic IS standard samples.

3. Results and discussion

3.1 Fragmentation patterns of the standards

By infusing solutions of each standard, their fragmentation patterns were obtained. Fragmentation patterns of one standard from each class were shown in **Figure 1**. Typical fragments of NAPEs and lyso-NAPEs include the fatty acid chains from sn-1 ($[R_1CO_2]^-$) and/or sn-2 ($[R_2CO_2]^-$), the phosphorylated N-fatty amide head group ($[R_3CONHCH_2CH_2OPO_3H]^-$). Typical fragments for pNAPEs and lyso-pNAPEs were similar, the only difference is the fragment from sn-1 ($[R_1O]^-$). The fragments that were used for the identification were listed in **Table 1**.

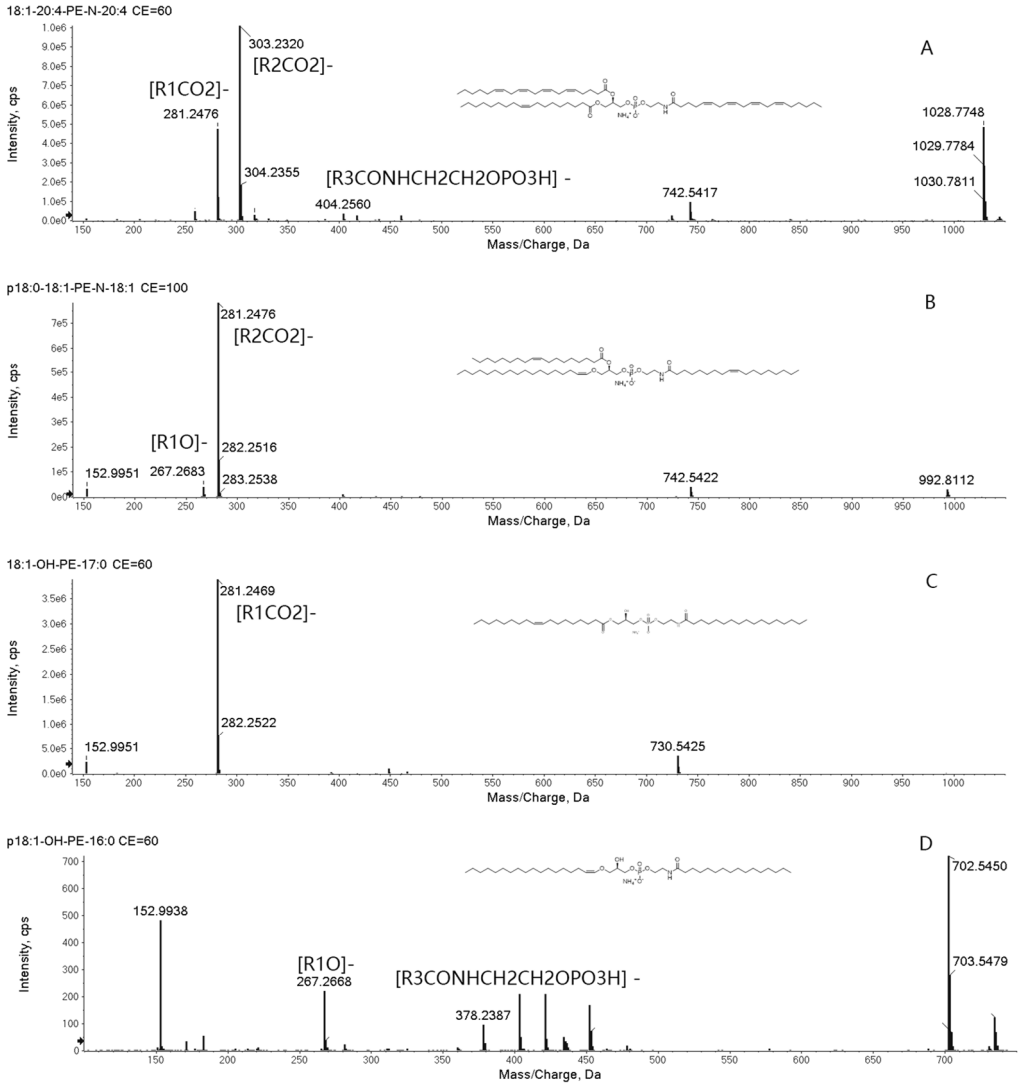

Figure 1. Typical fragmentation patterns of *N*-acyl-phosphatidylethanolamines, *N*-acyl-plasmalogen-phosphatidylethanolamines, 2-lyso-*N*-acyl-phosphatidylethanolamines and 2-lyso-*N*-acyl-plasmalogen-phosphatidylethanolamines A: 1-oleoyl-2-arachidonoyl-sn-glycero-3-phospho (*N*-arachidonoyl) ethanolamine (18:1, 20:4-PE-N-20:4); B: 1-(1Z-octadecenyl)-2-oleoyl-sn-glycero-3-phospho (*N*-oleoyl) ethanolamine (p18:0, 18:1-PE-N-18:1); C: 1-oleoyl-2-hydroxy-sn-glycero-3-phospho (*N*-heptadecanoyl) ethanolamine (18:1, OH-PE-N-16:0); D: 1-(1Z-octadecenyl)-2-hydroxy-sn-glycero-3-phospho (*N*-palmitoyl) ethanolamine (p18:0, OH-PE-N-16:0).

Table 1. Summary of the fragment ions, with Rx = 1, 2 or 3 according to the sn position.

Fragments	$[R_1CO_2]^-$	$[R_1O]^-$	$[R_2CO_2]^-$	$[R_3CONHCH_2CH_2OPO_3H]^-$	$[M\text{-}H - R_3CONHC_2H_4OH]^-$
NAPEs	Yes	NA	Yes	Yes	Not used
pNAPEs	NA	Yes	Yes	Yes	Not used
lyso-NAPEs	Yes	NA	NA	Yes	Not used
lyso-pNAPEs	NA	Yes	NA	Yes	Not used

* NAPEs (*N*-acyl-phosphatidylethanolamines), pNAPEs (*N*-acyl-plasmalogen-phosphatidylethanolamines), lyso-NAPEs (2-lyso-*N*-acyl-phosphatidylethanolamines), lyso-pNAPEs (2-lyso-N-acyl-plasmalogen-phosphatidylethanolamines), GP-NAEs (glycerol-phospho-acylethanolamines).

3.2 Development of sample preparation method and LC method

A liquid-liquid extraction method was used to concentrate the metabolites. Since these metabolites covered in this method had a wide range of lipophilicity, an extractant composed of butanol and MTBE (50:50, v:v) was used. Isopropanol and acetonitrile (50:50, v:v) was used and the agitation time was set to 15 minutes to get sufficient recovery for the pNAPEs. Notably, the reconstitution solvent was too strong for the eCBs in this mobile phase system and caused peak fronting. Thus in the autosampler, stack injection with 20 μL mobile phase A was applied.

A ternary gradient was used. The first part of the gradient used acetonitrile (MPB) to elute the eCBs and the FFAs. The second part of the gradient used isopropanol to elute out the lyso-NAPEs, lyso-pNAPEs, NAPEs and pNAPEs. From 8 to 10 minutes, the gradient was maintained so that the retention time were linearly correlated with carbon number and double bond number. Significant tailing of NAPEs and pNAPEs was observed when the separation was performed on a BEH C18 column (50 mm × 2.1 mm, 1.7 μm), which was solved by using a BEH C8 column (50 mm × 2.1 mm, 1.7 μm). It is commonly accepted that peak tailing can be caused by overloading of compounds and/or more than one retention mechanisms. While in this study, the amount of compound, the mobile phase and the end-capping of the columns were the same. The better peak shape on the C8 column might mean that different hydrophobicity of the alkyl groups can also result in different peak tailing factors.

3.3 Identification of metabolites with retention time mapping.

Calibration samples were used to determine the actual RT of each standard. Then the *b0*, *b1*, and *b2* for each class were calculated separately (**Table 2**). Predicted RT was calculated with the equation $RT = b0 + b1 \cdot carbon\ number + b2 \cdot double\ bond\ number$. For the standards, the deviation of the predicted RT from the actual RT was less than 0.1 min (**Table 2**). The identified metabolites were listed in **Table S3**. In total, 37 NAPEs, 32 pNAPEs, 33 lyso-NAPEs and 17 lyso-pNAPEs can be reliably quantified.

Analyte		Carbon number	Double bond number	b0	b1	b2	Calculated RT	Actual RT	RT deviation
NAPEs	18:1-18:1-PE-N-16:0	52	2	4.79	0.0895	-0.1275	9.189	9.21	0.021
	18:1-18:1-PE-N-17:0	53	2				9.278	9.30	0.0215
	18:1-18:1-PE-N-18:1	54	3				9.240	9.23	-0.0105
	18:1-18:1-PE-N-20:4	56	6				9.037	9.04	0.003
pNAPEs	p18:0-18:1-PE-N-16:0	52	1	5.17	0.089	-0.122	9.554	9.57	0.016
	p18:0-18:1-PE-N-17:0	53	1				9.643	9.68	0.037
	p18:0-18:1-PE-N-18:1	54	2				9.610	9.59	-0.02
	p18:0-18:1-PE-N-20:4	56	5				9.422	9.42	-0.002
lyso-NAPEs	18:1-OH-PE-N-16:0	34	1	5.02	0.0895	-0.1275	7.936	7.93	-0.0105
	18:1-OH-PE-N-17:0	35	1				8.025	8.02	-0.005
	18:1-OH-PE-N-18:1	36	2				7.987	7.98	-0.012
	18:1-OH-PE-N-20:4	38	5				7.783	7.79	0.0065
lyso-pNAPEs	p18:0-OH-PE-N-16:0	34	0	5.39	0.0895	-0.1275	8.305	8.28	-0.0255
	p18:0-OH-PE-N-17:0	35	0				8.395	8.41	0.015
	p18:0-OH-PE-N-18:1	36	1				8.357	8.32	-0.037
	p18:0-OH-PE-N-20:4	38	4				8.153	8.22	0.0665

Table 2. The correlation between retention time of analytes with their carbon number and double bond number. * NAPEs (*N*-acyl-phosphatidylethanolamines), pNAPEs (*N*-acyl-plasmalogen-phosphatidylethanolamines), lyso-NAPEs (2-lyso-*N*-acyl-phosphatidylethanolamines), lyso-pNAPEs (2-lyso-*N*-acyl-plasmalogen-phosphatidylethanolamines), RT (retention time).

3.4 Method validation

The optimized method was validated based on guidelines from FDA, EMA and ICH for bioanalytical method validation. Validation including linearity, precision, recovery and matrix effect was performed. The linearity and precision of analytes from each class are summarized in **Table 3**, recovery and matrix effect were summarized in **Figure 2**.

Linearity The square of correlation coefficient (R^2) values are all between 0.994 and 0.999 (significance F <0.05), and for at least 75% of the back calculated concentrations of analytes were within ±15% (20% for LLOQ) of the nominal value, which indicated that the linearity is good for all the analytes in the calibration range. Unexpectedly, different from pre-test results, 18:1-OH-PE-N-20:4 and p18:0-OH-PE-N-20:4 were not detected at endogenous levels, and peaks were only seen at higher than C6 levels, which might be caused by deteriorated sensitivity of the instrument.

Precision The within-run and between-run precisions samples were unspiked brain lysates (endogenous level, n=5) and spiked brain lysates (C8 level, n=5) over three separate batches. For most of the analytes, within-run and between-run precisions were lower than 15%, indicating good repeatability (**Table 3**). However, 2-AG showed a within-run variability of 21.8% at endogenous level, and very high between-run variability. Multiple reasons including high background at the transition of 2-AG and low-signal of the internal standard 2-AG-d8 may have caused the high variability. With these method, 2-AG can only be reported for samples that can be measured in one single batch and the data should be treated with caution.

Recovery and matrix effect were assessed at three different levels [low-level (C3), medium-level (C5), and high-level (C8), n=5 at each level]. For all the analytes except 2-AG, the recoveries ranged from 71.7% to 100.2%. Matrix effects ranged from 78.1% to 204.2% (**Figure 2**). For each analyte, the effect of recovery and matrix effect was consistent at three different levels. The exception was 2-AG-d8, which showed extremely low recovery at low and medium level, which may be the reason that caused the high variability. Minor ion suppression was observed for the NAEs, while significant ion enhancement was observed for FFAs, NAPEs and pNAPEs. The mechanism of ion suppression can be explained by the competition from the co-eluting matrix for the limited charges on the sprayed droplets formed by ESI[20,21]. Besides, co-eluting matrix may increase the viscosity and surface tension of the droplets and reduce the form of ions[20,21]. However, there has been limited

discussion on the mechanism of ion enhancement[21]. It has been reported that co-eluting phospholipids caused ion enhancement[22], while it is known that phospholipids act as surfactants. Therefore, based on the proposed mechanism of ion suppression, it is possible that phospholipids lowered the surface tension of ESI droplets and enhanced the ionization. More studies are required to look into the mechanism of ion enhancement. And with this method, when the samples showed significantly different pathologies, comparison of matrix effects among multiple sources should be done to exclude the possible impacts from ion enhancement.

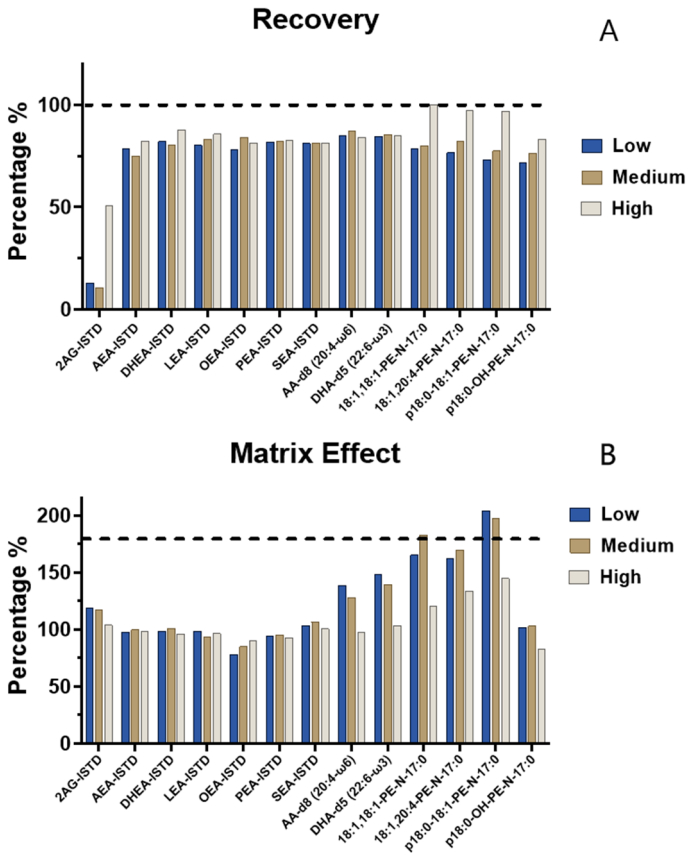

Figure 2. Recovery and matrix effect of internal standards in mice brain samples. Recovery and matrix effect values are expressed in percentages. (A) Recovery: higher values indicate better recoveries. (B) Matrix effect: values above 100% imply ion enhancement and below 100% imply ion suppression.

Table 3. Validation results: linearity, calibration range, within-day and between-day precision

Compound	R^2	LLOQ	ULOQ	Within-day precision (%)		Between-day precision (%)	
				medium	high	medium	high
AEA	0.999	1.95	250	6.9	1.7	6.1	4.5
DHEA	0.999	3.90	125	7.3	3.9	7.4	5.7
LEA	0.999	7.81	250	5.1	2.9	5.8	4.4
OEA	0.999	78.1	2500	4.2	6.3	26.1	7.4
PEA	0.999	78.1	2500	5.9	2.3	5.0	2.4
SEA	0.999	78.1	2500	3.9	2.0	3.4	2.8
DEA	0.999	3.91	250	12.1	5.1	12.7	4.8
DGLEA	0.998	7.81	250	2.3	3.7	3.1	5.2
2-AG	0.999	312.50	5000	21.8	7.4	34.2	57.3
Oleic acid (C18:1-ω9)	0.998	21100	337500	4.3	1.4	3.8	2.5
DGLA (C20:3-ω6)	0.999	2109	67500	4.6	2.8	6.5	4.4
AA (C20:4-ω6)	0.998	3100	101250	3.8	1.9	2.9	6.6
EPA (C20:5-ω3)	0.999	1600	50625	4.4	2.4	6.5	4.2
DHA (C22:6-ω3)	0.997	4219	67500	2.7	1.6	4.9	6.5
18:1, 18:1-PE-N-16:0	0.998	12.5	800	12.7	15.6	13.0	14.8
18:1, 18:1-PE-N-18:1	0.998	25	800	12.1	16.4	11.0	12.4
18:1, 18:1-PE-N-20:4	0.999	25	1600	16.5	17.4	14.2	15.1
p18:0, 18:1-PE-N-16:0	0.988	100	3200	3.5	3.3	5.0	6.3
p18:0, 18:1-PE-N-18:1	0.999	50	800	4.1	8.5	9.4	15.1
p18:0, 18:1-PE-N-20:4	0.998	5	160	21.0	11.6	26.6	17.5
18:1-OH-PE-N-16:0	0.997	10	160	2.4	2.5	15.7	7.9
18:1-OH-PE-N-18:1	0.994	10	160	8.6	2.0	16.0	4.0
18:1-OH-PE-N-20:4	-	-	-	-	1.5	-	7.1
p18:0-OH-PE-N-16:0	0.999	100	3200	5.9	1.9	6.5	5.0
p18:0-OH-PE-N-18:1	0.999	100	3200	5.8	7.5	15.2	14.2
p18:0-OH-PE-N-20:4	-	-	-	-	6.0	-	19.2

*R^2, correlation coefficient.

4 Conclusion

In this study, a LC-MS method that enabled the analysis of endocannabinoids and more than 100 related metabolites was developed. In mice brain samples, this method covered the major metabolic pathways of NAEs, including 37 NAPEs, 32 pNAPEs, 33 lyso-NAPEs and 17 lyso-pNAPEs. The coverage of the metabolic pathways of 2-AcGs was limited and required further improvement. The validation of the method showed acceptable variability for most of the analytes. This method enables the screening of enzymes potentially involved in the ECS, and moreover, the assessment of the impact of pharmacological modulation of the ECS-related enzymes.

References

1. Muccioli, G. G. Endocannabinoid biosynthesis and inactivation, from simple to complex. *Drug Discovery Today* vol. 15 474–483 (2010).
2. Hillard, C. J. Circulating Endocannabinoids: From Whence Do They Come and Where are They Going? *Neuropsychopharmacology* **43**, 155–172 (2018).
3. Matsuda, L. A., Lolait, S. J., Brownstein, M. J., Young, A. C. & Bonner, T. I. Structure of a cannabinoid receptor and functional expression of the cloned cDNA. *Nature* **346**, 561–564 (1990).
4. Devane, W. A. *et al.* Isolation and structure of a brain constituent that binds to the cannabinoid receptor. *Science* **258**, 1946–1949 (1992).
5. Astarita, G., Ahmed, F. & Piomelli, D. Identification of biosynthetic precursors for the endocannabinoid anandamide in the rat brain. *Journal of Lipid Research* **49**, 48–57 (2008).
6. Cristino, L., Bisogno, T. & di Marzo, V. Cannabinoids and the expanded endocannabinoid system in neurological disorders. *Nat Rev Neurol* **16**, 9–29 (2020).
7. Tsuboi, K. *et al.* Enzymatic formation of N-acylethanolamines from N-acylethanolamine plasmalogen through N-acylphosphatidylethanolamine-hydrolyzing phospholipase D-dependent and -independent pathways. *Biochimica et Biophysica Acta - Molecular and Cell Biology of Lipids* **1811**, 565–577 (2011).
8. Ogura, Y., Parsons, W. H., Kamat, S. S. & Cravatt, B. F. A calcium-dependent acyltransferase that produces N-Acyl phosphatidylethanolamines. *Nature Chemical Biology* **12**, 669–671 (2016).
9. Murataeva, N., Straiker, A. & MacKie, K. Parsing the players: 2-arachidonoylglycerol synthesis and degradation in the CNS. *British Journal of Pharmacology* **171**, 1379 (2014).
10. Bisogno, T. *et al.* Cloning of the first sn1-DAG lipases points to the spatial and temporal regulation of endocannabinoid signaling in the brain. *J Cell Biol* **163**, 463–468 (2003).
11. van Esbroeck, A. C. M. *et al.* Identification of α,β-Hydrolase Domain Containing Protein 6 as a Diacylglycerol Lipase in Neuro-2a Cells. *Frontiers in Molecular Neuroscience* **12**, (2019).
12. Kathuria, S. *et al.* Modulation of anxiety through blockade of anandamide hydrolysis. *Nature Medicine* **9**, 76–81 (2003).
13. Stone, N. L. *et al.* An analysis of endocannabinoid concentrations and mood following singing and exercise in healthy volunteers. *Frontiers in Behavioral Neuroscience* **12**, (2018).

14. Zou, S. & Kumar, U. Cannabinoid receptors and the endocannabinoid system: Signaling and function in the central nervous system. *International Journal of Molecular Sciences* vol. 19 (2018).
15. Gaetani, S., Cuomo, V. & Piomelli, D. Anandamide hydrolysis: A new target for anti-anxiety drugs? *Trends in Molecular Medicine* **9**, 474–478 (2003).
16. Řezanka, T., Vítová, M., Lukavský, J. & Sigler, K. Lipidomic Study of Precursors of Endocannabinoids in Freshwater Bryozoan Pectinatella magnifica. *Lipids* **53**, 413–427 (2018).
17. Röhrig, W., Achenbach, S., Deutsch, B. & Pischetsrieder, M. Quantification of 24 circulating endocannabinoids, endocannabinoid-related compounds, and their phospholipid precursors in human plasma by UHPLC-MS/MS. *Journal of Lipid Research* **60**, 1475–1488 (2019).
18. Řezanka, T., Vítová, M., Lukavský, J. & Sigler, K. Lipidomic Study of Precursors of Endocannabinoids in Freshwater Bryozoan Pectinatella magnifica. *Lipids* **53**, 413–427 (2018).
19. Triebl, A., Weissengruber, S., Trötzmüller, M., Lankmayr, E. & Köfeler, H. Quantitative analysis of N-acylphosphatidylethanolamine molecular species in rat brain using solid-phase extraction combined with reversed-phase chromatography and tandem mass spectrometry. *Journal of Separation Science* **39**, 2474–2480 (2016).
20. Antignac, J.-P. *et al.* The ion suppression phenomenon in liquid chromatography-mass spectrometry and its consequences in the field of residue analysis. *Analytica Chimica Acta* **529**, 129–136 (2005).
21. van Eeckhaut, A., Lanckmans, K., Sarre, S., Smolders, I. & Michotte, Y. Validation of bioanalytical LC-MS/MS assays: Evaluation of matrix effects. *Journal of Chromatography B: Analytical Technologies in the Biomedical and Life Sciences* **877**, 2198–2207 (2009).
22. OA, I., MS, H., MY, E., A, S. & H, T. K. Monitoring phospholipids for assessment of ion enhancement and ion suppression in ESI and APCI LC/MS/MS for chlorpheniramine in human plasma and the importance of multiple source matrix effect evaluations. *J Chromatogr B Analyt Technol Biomed Life Sci* **875**, 333–343 (2008).

Supplementary material

Table S1. Concentration of compounds in standard stock solution I, II, and III.

	Molecular weight	Concentration (μM)
1-Arachidonoyl Glycerol	378.54	13.5
2-Arachidonoyl Glycerol	378.54	13.5
Arachidonoyl Ethanolamide	347.54	13.5
Docosahexaenoyl Ethanolamide	371.56	13.5
Linoleoyl Ethanolamide	323.51	13.5
Oleoyl Ethanolamide	325.53	13.5
Palmitoyl Ethanolamide	299.49	27
Stearoyl Ethanolamide	327.6	13.5
Docosatetraenoyl Ethanolamide	375.6	1.35
Dihomo-γ-Linolenoyl Ethanolamide	349.55	1.35
O-Arachidonoyl Ethanolamine	347.54	13.5
2-Linoleoyl Glycerol	354.52	135
1-Linoleoyl Glycerol	354.52	135
2-Oleoyl Glycerol	356.55	135
Eicosapentaenoyl Ethanolamide	345.52	1.35
Palmitoleoyl Ethanolamide	297.48	13.5
5(Z),8(Z),11(Z)-Eicosatrienoic Acid Ethanolamide	349.55	1.35
Pentadecanoyl Ethanolamide	285.46	1.35
α-Linolenoyl Ethanolamide	321.5	1.35
Standard stock solution II		
α-Linolenic Acid (C18:3-w3)	278.44	1350
γ-Linolenic Acid (C18:3-w6)	278.44	1350
Linoleic Acid (C18:2-w6)	280.45	4050
Eicosapentaenoic Acid (C20:5-w3)	302.46	1012.5
Arachidonic Acid (C20:4-w6)	304.47	2025
Dihomo-γ-Linolenic Acid (C20:3-w6)	306.49	675
Mead acid (C20:3-w9)	306.49	675
Docosahexaenoic Acid (C22:6-w3)	328.5	2700
cis-4,10,13,16-Docosatetraenoic Acid (C22:4-w6)	332.53	675
Oleic acid (C18:1-w9)	282.47	6750
Standard stock solution III		
18:1, 18:1-PE-N-20:4	1053.85	10
18:1, 18:1-PE-N-16:0	999.49	10
18:1, 18:1-PE-N-18:1	1026.79	10
p18:0, 18:1-PE-N-20:4	1047.86	1
p18:0, 18:1-PE-N-16:0	986.883	10
p18:0, 18:1-PE-N-18:1	1011.544	10
18:1-OH-PE-N-20:4	783.085	1
18:1-OH-PE-N-16:0	735.041	2
18:1-OH-PE-N-18:1	761.079	2
p18:0-OH-PE-N-20:4	769.102	20
p18:0-OH-PE-N-16:0	721.058	20
p18:0-OH-PE-N-18:1	747.096	20

Table S2. Concentration of compounds in internal standard stock solution A and B.

IS standard stock solution A	Molecular weight	Concentration (μM)
Arachidonic Acid-d_8	312.5	50
Docosahexaenoic Acid-d_5	333.5	25
Linoleic Acid-d_4	284.5	100
Oleic Acid-d_{17}	298.2	100
2-Arachidonoyl Glycerol-d_8	386.6	50
Arachidonoyl Ethanolamide-d_8	355.6	5
Docosahexaenoyl Ethanolamide-d_4	375.6	5
Linoleoyl Ethanolamide-d_4	327.5	5
Oleoyl Ethanolamide-d_4	329.6	5
Palmitoyl Ethanolamide-d_4	303.5	5
Stearoyl Ethanolamide-d_3	330.6	5
IS standard stock solution B		
18:1, 18:1-PE-N-17:0	1031.52	2.5
p18:0, 18:1-PE-N-17:0	1004.419	2.5
18:1-OH-PE-N-17:0	749.068	2.5
p18:0-OH-PE-N-17:0	735.085	2.5

Table S3. Identified metabolites with retention time mapping in mice brain tissues.

Name	Expected RT	Actual RT	RT delta	Precursor	[R1CO2]-/[R1CO]-	[R2CO2]-	[R3CONHCH2CH2OPO3H]-
(16:1, 16:1)-PE-N-18:1	8.87	8.91	0.04	950.7	253.22	253.22	404.2
(16:1, 18:1)-PE-N-16:0	9	9.06	0.06	952.7	253.23	281.21	378.2
(16:0, 18:1)-PE-N-16:0	9.13	9.19	0.06	954.7	255.23	281.21	378.2
(16:0, 16:0)-PE-N-20:4	8.92	9.00	0.08	976.7	255.21	255.21	426.2
(16:1, 18:2)-PE-N-18:1	8.92	8.92	0.00	976.7	253.23	279.21	404.2
(16:0, 18:2)-PE-N-18:1	9.05	9.05	0.00	978.7	255.23	279.21	404.2
(18:2, 18:1)-PE-N-16:0	9.05	9.05	0.00	978.7	279.21	281.21	378.2
(16:0, 18:1)-PE-N-18:1	9.18	9.21	0.03	980.8	255.23	281.21	404.2
(18:0, 18:2)-PE-N-16:0	9.18	9.22	0.04	980.8	279.22	283.32	378.2
(18:0, 18:1)-PE-N-16:0	9.31	9.39	0.08	982.8	283.22	281.22	378.2
(16:0, 18:2)-PE-N-20:4	8.85	8.91	0.06	1000.7	255.22	279.21	426.2
(16:0, 20:4)-PE-N-18:1	8.98	9.01	0.03	1002.7	255.21	303.22	404.2
(16:0, 20:4)-PE-N-18:0	9.1	9.13	0.03	1004.8	255.21	303.22	406.2
(18:2, 18:2)-PE-N-18:0	9.1	9.07	-0.03	1004.8	279.21	279.21	406.2
(18:1, 18:2)-PE-N-18:1	9.1	9.07	-0.03	1004.8	281.21	279.21	404.2
(18:0, 20:4)-PE-N-16:0	9.1	9.17	0.07	1004.8	283.31	303.22	378.2
(18:1, 20:3)-PE-N-16:0	9.1	9.07	-0.03	1004.8	281.21	305.22	378.2
(18:0, 18:1)-PE-N-18:2	9.23	9.26	0.03	1006.8	281.21	283.31	402.2

(18:1, 18:1)-PE-N-18:0	9.36	9.39	0.03	1008.8	281.21	281.21	406.2
(18:0, 18:1)-PE-N-18:1	9.36	9.42	0.06	1008.8	281.21	283.33	404.2
(18:1, 18:2)-PE-N-20:4	8.9	8.90	0.00	1026.7	279.21	281.21	426.2
(16:0, 18:0)-PE-N-22:6	9.03	9.06	0.03	1028.8	255.21	283.31	450.2
(18:0, 18:2)-PE-N-20:4	9.03	9.04	0.01	1028.8	283.31	279.21	426.2
(18:2, 20:4)-PE-N-18:0	9.03	9.06	0.03	1028.8	279.21	303.21	406.2
(18:1, 20:4)-PE-N-18:1	9.03	9.02	-0.01	1028.8	281.21	303.21	404.2
(18:0, 20:4)-PE-N-18:2	9.03	9.04	0.01	1028.8	283.31	303.21	402.2
(18:0, 18:1)-PE-N-20:4	9.15	9.20	0.05	1030.8	283.31	281.21	426.2
(18:1, 20:4)-PE-N-18:0	9.15	9.17	0.02	1030.8	281.21	303.21	406.2
(18:1, 20:3)-PE-N-18:1	9.15	9.18	0.03	1030.8	281.21	305.21	404.2
(18:0, 20:3)-PE-N-18:1	9.28	9.21	-0.07	1032.8	283.31	305.21	404.2
(18:0, 20:4)-PE-N-20:4	8.95	9.01	0.06	1052.8	283.2	303.21	426.3
(18:0, 20:3)-PE-N-20:4	9.08	9.08	0.00	1054.8	283.32	305.2	426.3
(18:0, 22:6)-PE-N-20:4	8.87	8.93	0.06	1076.8	327.21	283.2	426.3
p16:0-18:1-PE-N-16:0	9.35	9.35	0.00	938.8	239.2	281.2	378.2
p18:1-16:0-PE-N-16:0	9.35	9.34	-0.01	938.8	265.2	255.2	378.2
p18:1-18:1-PE-N-16:0	9.4	9.35	-0.05	964.8	265.2	281.2	378.2
p16:0-18:1-PE-N-18:1	9.4	9.37	-0.03	964.8	239.2	281.2	404.3
p18:0-18:1-PE-N-16:0	9.53	9.57	0.04	966.8	267.2	281.2	378.2
p16:0-18:1-PE-N-18:0	9.53	9.55	0.02	966.8	239.2	281.2	406.3
p16:1-18:1-PE-N-20:4	9.07	8.89	-0.18	984.8	237.2	281.2	426.2
p16:1-20:4-PE-N-18:0	9.2	9.28	0.08	986.8	237.2	303.2	406.3
p18:1-16:0-PE-N-20:4	9.2	9.17	-0.03	986.8	265.2	255.2	426.2
p18:0-20:4-PE-N-16:0	9.33	9.30	-0.03	988.8	267.2	303.2	378.2
p16:0-20:4-PE-N-18:0	9.33	9.28	-0.05	988.8	239.2	303.2	406.3
p18:0-18:1-PE-N-18:2	9.45	9.48	0.03	990.8	267.2	281.2	402.2
p18:1-18:1-PE-N-18:1	9.45	9.35	-0.10	990.8	265.2	281.2	404.3
p18:0-18:1-PE-N-18:1	9.58	9.60	0.02	992.8	267.2	281.2	404.3
p18:1-18:1-PE-N-18:0	9.58	9.57	-0.01	992.8	265.2	281.2	406.3
p16:1-18:0-PE-N-22:6	9.12	9.05	-0.07	1010.8	237.2	281.2	450.2
p18:0-22:6-PE-N-16:0	9.25	9.19	-0.06	1012.8	267.2	327.2	378.2
p18:0-20:4-PE-N-18:2	9.25	9.04	-0.21	1012.8	267.2	303.2	402.2
p20:4-18:0-PE-N-18:2	9.25	9.28	0.03	1012.8	287.2	283.3	402.2
p20:4-18:1-PE-N-18:1	9.25	9.13	-0.12	1012.8	287.2	281.2	404.3
p16:0-22:6-PE-N-18:0	9.25	9.19	-0.06	1012.8	255.2	327.2	406.3
p20:5-18:1-PE-N-18:0	9.25	9.18	-0.07	1012.8	285.2	281.2	406.3
p18:1-18:1-PE-N-20:4	9.25	9.18	-0.07	1012.8	265.2	281.2	426.2
p18:0-20:4-PE-N-18:1	9.38	9.31	-0.07	1014.8	267.2	303.2	404.3
p18:1-20:4-PE-N-18:0	9.38	9.31	-0.07	1014.8	265.2	303.2	406.3
p20:3-20:4-PE-N-18:2	9.05	8.88	-0.17	1034.8	289.2	303.2	402.2
p18:1-20:4-PE-N-20:4	9.05	8.97	-0.08	1034.8	265.2	303.2	426.2
p20:4-18:1-PE-N-22:6	8.97	8.90	-0.07	1058.8	287.2	281.2	450.2
16:1-OH-PE-16:0	7.78	7.71	-0.07	688.49	253.22		
16:0-OH-PE-16:0	7.9	7.89	-0.01	690.51	255.23		

16:1-OH-PE-18:2	7.7	7.68	-0.02	712.49	253.22
16:1-OH-PE-18:1	7.83	7.75	-0.08	714.51	253.22
16:0-OH-PE-18:2	7.83	7.75	-0.08	714.51	255.23
18:2-OH-PE-16:0	7.83	7.74	-0.09	714.51	279.23
16:0-OH-PE-18:1	7.96	7.94	-0.02	716.52	255.23
18:1-OH-PE-16:0	7.96	7.94	-0.02	716.52	281.25
16:0-OH-PE-18:0	8.08	8.15	0.07	718.54	255.23
18:0-OH-PE-16:0	8.08	8.12	0.04	718.54	283.26
18:1-OH-PE-17:0	8.05	8.04	-0.01	730.54	281.25
16:0-OH-PE-20:4	7.75	7.74	-0.01	738.51	255.23
18:2-OH-PE-18:2	7.75	7.76	0.01	738.51	279.23
20:4-OH-PE-16:0	7.75	7.72	-0.03	738.51	303.23
18:3-OH-PE-18:0	7.88	7.81	-0.07	740.52	277.22
18:2-OH-PE-18:1	7.88	7.78	-0.10	740.52	279.23
18:1-OH-PE-18:1	8.01	7.98	-0.03	742.54	281.25
18:0-OH-PE-18:2	8.01	8.01	0.00	742.54	283.26
18:1-OH-PE-18:0	8.13	8.13	0.00	744.55	281.25
18:0-OH-PE-18:1	8.13	8.19	0.06	744.55	283.26
18:0-OH-PE-18:0	8.26	8.35	0.09	746.57	283.26
16:0-OH-PE-22:6	7.68	7.72	0.04	762.51	255.23
18:1-OH-PE-20:4	7.8	7.78	-0.02	764.52	281.25
20:4-OH-PE-18:1	7.8	7.75	-0.05	764.52	303.23
18:0-OH-PE-20:4	7.93	7.99	0.06	766.54	283.26
20:4-OH-PE-18:0	7.93	7.94	0.01	766.54	303.23
18:2-OH-PE-22:6	7.6	7.78	0.18	786.51	279.23
18:1-OH-PE-22:6	7.73	7.72	-0.01	788.52	281.25
18:0-OH-PE-22:6	7.85	7.84	-0.01	790.54	283.26
p16:0-OH-PE-16:0	8.13	8.04	-0.09	674.51	239.2
p18:0-OH-PE-16:0	8.31	8.27	-0.04	702.54	267.3
p16:0-OH-PE-18:0	8.31	8.27	-0.04	702.54	239.2
p16:1-OH-PE-18:0	8.18	8.06	-0.12	700.53	237.2
p18:0-OH-PE-18:0	8.48	8.63	0.15	730.57	267.3
p18:1-OH-PE-18:0	8.36	8.27	-0.09	728.56	265.3
p16:0-OH-PE-18:1	8.18	8.06	-0.12	700.53	239.2
p18:0-OH-PE-18:1	8.36	8.30	-0.06	728.56	267.3
p18:1-OH-PE-18:1	8.23	8.28	0.05	726.54	265.3
p18:0-OH-PE-18:2	8.23	8.21	-0.02	726.54	267.3
p16:0-OH-PE-20:4	8.15	8.05	-0.10	722.51	239.2
p18:1-OH-PE-20:4	8.15	8.09	-0.06	748.54	265.3
p18:0-OH-PE-22:6	8.08	8.09	0.01	774.54	267.3
p22:6-OH-PE-22:6	7.67	7.74	0.07	818.51	311.2